

University of Arkansas, Fayetteville

ScholarWorks@UARK

---

Chemistry & Biochemistry Undergraduate  
Honors Theses

Chemistry & Biochemistry

---

5-2023

## Detection of Nitrogen Dioxide via Graphene-Enhanced Raman Scattering

Spencer Hazeslip

University of Arkansas, Fayetteville

Follow this and additional works at: <https://scholarworks.uark.edu/chbcuht>



Part of the [Analytical Chemistry Commons](#), [Environmental Monitoring Commons](#), [Materials Chemistry Commons](#), and the [Physical Chemistry Commons](#)

---

### Citation

Hazeslip, S. (2023). Detection of Nitrogen Dioxide via Graphene-Enhanced Raman Scattering. *Chemistry & Biochemistry Undergraduate Honors Theses* Retrieved from <https://scholarworks.uark.edu/chbcuht/45>

This Thesis is brought to you for free and open access by the Chemistry & Biochemistry at ScholarWorks@UARK. It has been accepted for inclusion in Chemistry & Biochemistry Undergraduate Honors Theses by an authorized administrator of ScholarWorks@UARK. For more information, please contact [scholar@uark.edu](mailto:scholar@uark.edu), [uarepos@uark.edu](mailto:uarepos@uark.edu).

# **Detection of Nitrogen Dioxide via Graphene-Enhanced Raman Scattering**

An Honors Thesis submitted in partial fulfillment of the requirements of Honors Studies in  
Chemistry

By

Spencer Hazeslip

Spring 2023

Department of Chemistry and Biochemistry

J. William Fulbright College of Arts and Sciences

**The University of Arkansas**

## **Acknowledgments:**

I would like to express my sincere gratitude to my advisor, Dr. Maggie He, for her guidance and support throughout the research process. Dr. He's dedication and willingness to answer my countless questions have been instrumental in shaping my understanding of the research topic. I am thankful for the opportunity to learn from her and for the time she has invested in my growth as a researcher.

I would like to express my appreciation to the University of Arkansas Honors College for providing me with the opportunity to focus my efforts on my academic and research pursuits. It has enabled me to delve deeply into my interests and work closely with faculty mentors who have helped me grow as a scholar. The resources and opportunities that the Honors College has provided me have been instrumental in shaping my academic journey.

Lastly, I want to thank my family for their unwavering love and support. Their endless encouragement has been key in helping me pursue my academic and personal goals with determination.

## **Contents**

Acknowledgments: .....	2
Abstract: .....	3
Introduction.....	4
Experimental Details.....	7
Sample preparation.....	7
Raman measurement .....	7
Results and Discussion .....	8
CuPc-coated graphene.....	8
CuTTPc-coated graphene.....	10
Initial Attempts at NO <sub>2</sub> Exposure.....	13
Real-time Detection of NO <sub>2</sub> .....	16
Sensing Mechanism.....	23
Conclusion and Future Work .....	24
References:.....	25

**Abstract:**

This paper presents the development of a nitrogen dioxide (NO<sub>2</sub>) sensor that utilizes the phenomenon of graphene-enhanced Raman scattering (GERS). The sensor consists of monolayer graphene on a silicon wafer, functionalized noncovalently with Copper(II) 2,9,16,23-tetra-tert-butyl-29H,31H-phthalocyanine (CuTTPc) via the solution soaking method. A custom sensing chamber was constructed to enable Raman spectra to be collected during NO<sub>2</sub> exposure. The response of the sensor was found to be linear between 10 and 100 ppm NO<sub>2</sub>, indicating that it could be used for both detection and quantification. Furthermore, the sensor was shown to be reusable after exposure to 10 ppm NO<sub>2</sub>. These results demonstrate the potential of GERS-based NO<sub>2</sub> sensors for practical applications in environmental monitoring and safety management.

## Introduction

Raman spectroscopy is a method of analysis that uses the inelastic scattering of photons to determine the structure of molecules and materials. When light hits an object, there are a variety of interactions that could occur such as reflection, absorption, transmission, or scattering. Raman scattering occurs when light scattered by matter has different frequencies than the incident light. The light scattering process was named after physicist C. V. Raman, who received the Nobel Prize in Physics in 1930 for his discovery. The Raman scattering process occurs as follow: (1) a sample is irradiated by a laser of specific wavelength (also known as the excitation wavelength), (2) an electron in the ground state absorbs a photon and promotes to an excited state (if the excitation wavelength is far away from the molecules absorption band, the excited state is a virtual state), and (3) immediate relaxation followed by reemission of a photon (**Figure 1**).<sup>1</sup>

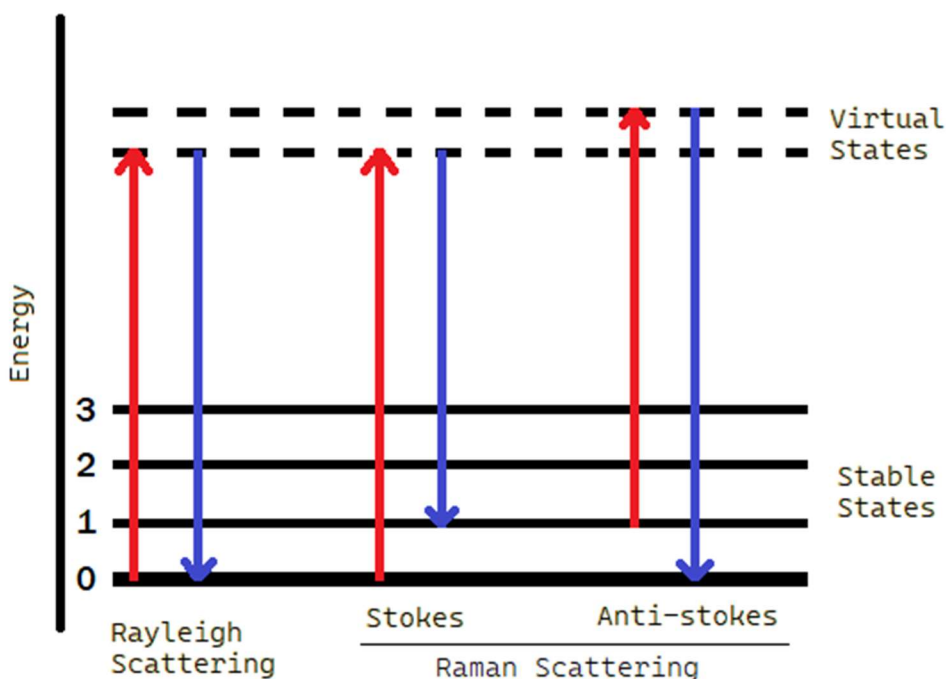


**Figure 1.** Jablonski diagram demonstrating the mechanism for different types of scattering.

Most of the electrons are excited from and returned to the same ground vibrational level. This type of scattering is known as Rayleigh scattering and the scattered photons have the same wavelength or frequency as the incident photons. Photons that are inelastically scattered, meaning that the scattered photons have a different wavelength or frequency than the incident light, is called Raman scattering. Specifically, when the electron returns to a higher ground vibrational level than

it was excited from, then the scattered photon will be lower in energy than the excitation photon and it is known as a Stokes shift. Conversely, an anti-Stokes shift occurs when the electron falls to a lower ground vibrational level than it was excited from, resulting in a higher energy photon being scattered.<sup>1</sup> Since most electrons are in the lowest ground vibration level when they interact with a photon (and can therefore not fall to a lower energy stable state than they started in), Stokes shifts are much more frequent than anti-Stokes shifts. For this reason, Raman spectroscopy typically only measures scattered photons with lower energy than the incident light.

Raman spectroscopy measures the frequency shift between the scattered radiation and the incident radiation. This frequency shift is often denoted as Raman shift using wavenumber ( $\text{cm}^{-1}$ ) as the unit. Since frequency modulation is specific to molecular vibrations, the Raman shifts are characteristic of molecular structure and presence of specific functional groups.<sup>1</sup>

For this reason, Raman and infrared spectroscopy are often considered complementary techniques for molecular characterization. While IR-active vibrational modes require a change in dipole moment, Raman-active vibrational modes require a change in bond polarizability. Many vibrational modes that are inactive or weak in IR often have strong Raman signals.

Because photon-electron interactions are relatively rare, the intensity of scattered light is very low compared to its source, and only a small fraction of scattered light is scattered inelastically. As a result, the sensitivity of Raman spectroscopy is inherently very weak, with a signal intensity less than 0.001% of the intensity of the source.

Fortunately, there are ways to improve the intensity of Raman scattering. In the 1970s, it was found that adsorbing molecules onto a rough surface of metals such as silver, gold or copper significantly enhances the Raman signal. This effect is called surface-enhanced Raman scattering (SERS) and is predominantly the result of electromagnetic interactions between the analyte and the substrate, although chemical interactions play a minor role in some cases.<sup>2</sup> The enhancement of Raman signals by SERS is substantial, making it a practical and sensitive method for molecular analysis. However, a rough or highly engineered surface is required for this technique to work, resulting in non-homogeneous enhancement.<sup>3</sup>

Graphene-enhanced Raman scattering (GERS) was first described by Ling et al<sup>4</sup> in 2010. Graphene is a material consisting of a monolayer of interconnected  $\text{sp}^2$  carbon in a hexagonal

manner. Unlike SERS, which relies on rough, plasmonic metal surfaces, GERS delivers a homogeneous surface that leads to high stability, reproducibility, and quantifiability.<sup>4,5</sup> Because of the flat surface and since the surface plasmon on graphene appears in the terahertz range, GERS must rely on the chemical method of enhancement, which arises from charge transfer between graphene and the analyte. Charge transfer is maximized by having the right balance between the analyte's HOMO and LUMO, the Fermi level of graphene, and the energy of the excitation laser.<sup>3</sup> Using graphene as a substrate for Raman spectroscopy dramatically increases signal intensity and reveals features that are not visible on other substrates.

Nitrogen dioxide is a toxic environmental pollutant. In water, it forms nitric acid and nitric oxide, thus contributing to acid rain. When inhaled, it irritates mucus membranes can even cause death in high concentrations.<sup>6</sup>  $\text{NO}_2$  is primarily produced through combustion of fuel in industry, power plants, combustion engine powered vehicles, and gas stoves. Monitoring the presence and concentration of this gas is important for determining environmental safety.

It is proposed that a GERS-based sensor for the detection of nitrogen dioxide can be created through the functionalization of graphene with a Raman-active molecule that interacts with nitrogen dioxide. Copper phthalocyanine is a prime candidate as it has several Raman-active vibrational modes and has been reported to form a charge-transfer complex (CTC) with nitrogen dioxide.<sup>7</sup>

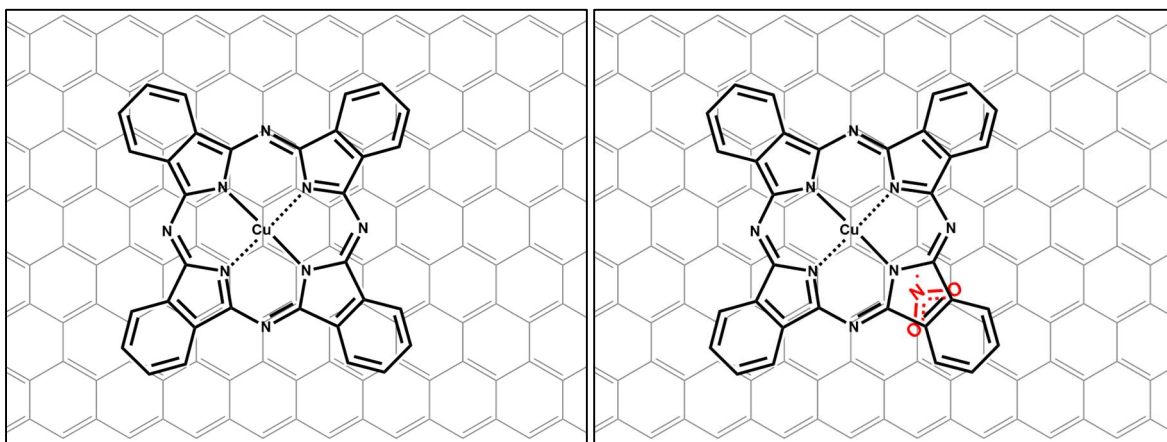


**Figure 2.** Structure of copper phthalocyanine on graphene before and after interaction with  $\text{NO}_2$ .<sup>8</sup>

Functionalization can be achieved either covalently or non-covalently. With non-covalent functionalization, the detector molecule is adsorbed to the surface of the graphene as shown in

**Figure 2.** This can be achieved through a variety of techniques: thermal/vacuum deposition, spin coating, Langmuir-Blodgett deposition, or solution soaking.<sup>4</sup> Covalent functionalization requires a reaction with the graphene lattice that creates sp<sup>3</sup> carbons to which the detector molecule would then be covalently bonded. This requires the synthesis of appropriate reagents and covalent modification of graphene, but may result in a more evenly functionalized surface and eliminate the risk of inadvertently rinsing the detector molecule from the graphene.

This project will demonstrate the detection of nitrogen dioxide through the functionalization of a graphene wafer with a Raman-active molecule that is capable of forming a charge transfer complex with NO<sub>2</sub>. Following the development of a functionalization technique and demonstration of NO<sub>2</sub> detection, quantification of NO<sub>2</sub> concentration, sensor limit of detection, sensor reusability, mechanism of sensor detection, and sensor selectivity will also be explored.

## **Experimental Details**

### **Sample preparation**

Graphene samples coated with copper phthalocyanine (CuPc) or Copper(II) 2,9,16,23-tetra-*tert*-butyl-29*H*,31*H*-phthalocyanine (CuTTPc) were prepared via solution soaking process. Solutions with concentrations of 10<sup>-3</sup> M to 10<sup>-7</sup> M for soaking were prepared by dissolving CuPc or CuTTPc in dichloromethane. Monolayer graphene on silicon wafer was purchased from Grolltex and was cut into ~ 5 mm x 5 mm pieces for sample preparation and Raman measurements. Graphene samples coated with CuPc or CuTTPc were prepared by immersing monolayer graphene in the corresponding dye dilutions for the indicated amount of time, then removed and dried under nitrogen.

### **Raman measurement**

Raman spectra were measured using a Renishaw inVia confocal Raman microscope. A 633 nm or 532 nm laser was used for excitation. Samples were placed under a 100x objective and full range spectra were obtained for each of the samples to determine both Raman scattering intensity and sample homogeneity. Realtime NO<sub>2</sub> sensing measurements were recorded with a 633 nm laser, 20x objective, 5-second laser exposure time, 50% power, and one accumulation every 5 seconds, from 1235–1752 cm<sup>-1</sup>. The NO<sub>2</sub> source was 100 ppm NO<sub>2</sub> in air (20.9% oxygen in nitrogen).



## Results and Discussion

### CuPc-coated graphene

We begin our study by coating the surface of graphene with different concentrations of CuPc via solution soaking (see Sample preparation). CuPc has six characteristic vibrational modes, 680, 750, 1140, 1340, 1450, and 1530  $\text{cm}^{-1}$ . The 650 and 750  $\text{cm}^{-1}$  modes are vibrations associated with the macrocycle and the four modes between 1140 and 1531  $\text{cm}^{-1}$  are associated with the vibrations of the isoindole ring.<sup>9</sup>

The Raman enhancement effect from graphene was evident as all of the expected Raman shifts for CuPc were clearly observed on graphene samples coated with CuPc (**Figure 3, left**). Using the most prominent CuPc peak, located at 1529  $\text{cm}^{-1}$ , as a metric, it was demonstrated that Raman signal intensity correlates positively with the concentration of CuPc solution used in the soaking procedure up to  $10^{-4}$  M, after which  $10^{-3}$  M shows an intensity decrease (**Figure 3, right**).

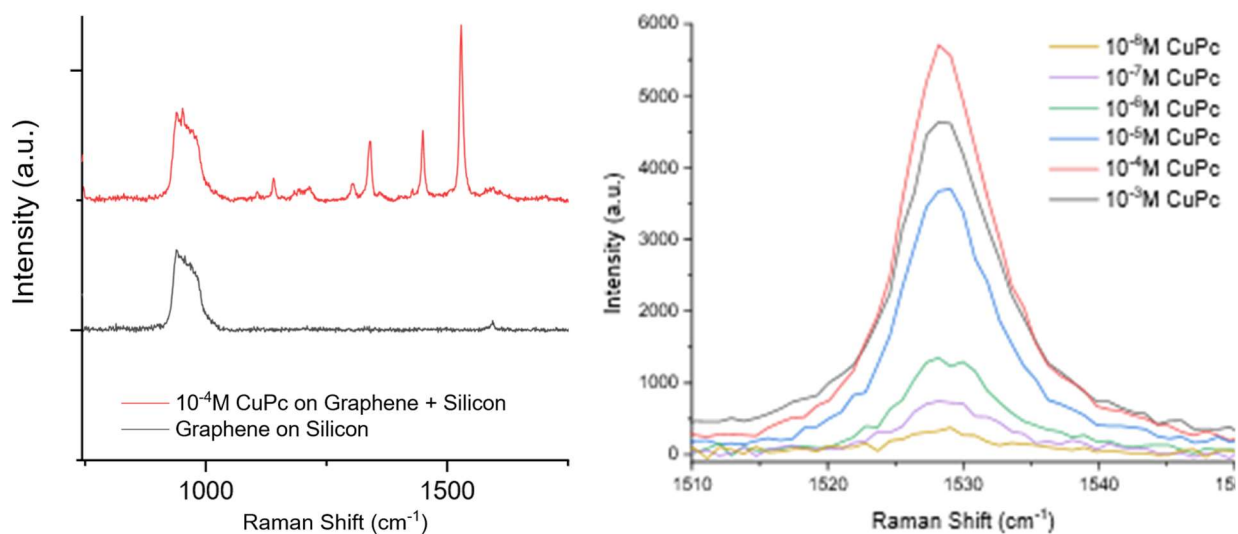


**Figure 3.** Raman spectra of CuPc on graphene showing the characteristic CuPc modes (left). Raman spectra showing the change in peak intensity for graphene prepared with various concentrations of CuPc in dichloromethane (right).

There were concerns that at higher concentrations since multi-layer deposition may occur and compromise surface homogeneity. To determine whether this was occurring, surface intensity maps were created using the Renishaw WiRE software. These maps show the intensity of the 1529

$\text{cm}^{-1}$  peak at 100 locations for a  $10\ \mu\text{m} \times 10\ \mu\text{m}$  area of the CuPc-functionalized graphene wafer. Maps were created for graphene samples prepared using  $10^{-4}\ \text{M}$  CuPc and  $10^{-5}\ \text{M}$  CuPc solutions.

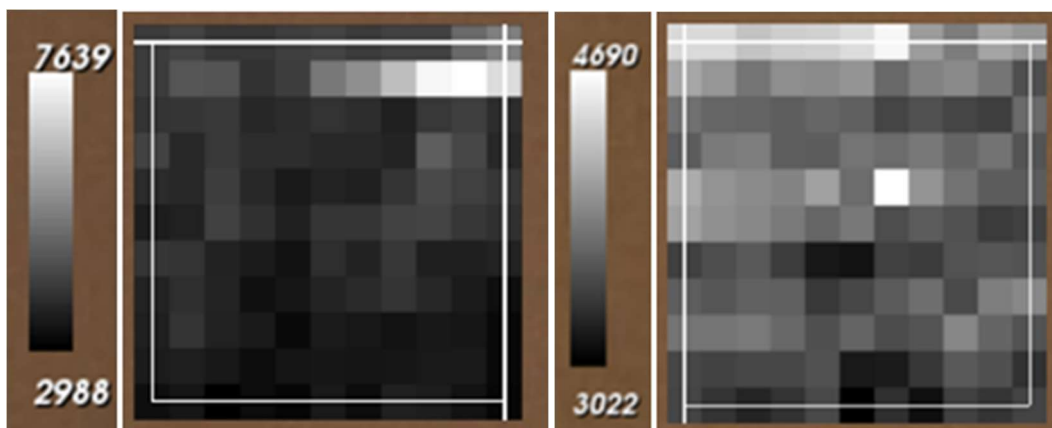


**Figure 4.** Raman intensity surface maps of graphene wafers prepared with  $10^{-4}\ \text{M}$  CuPc (left) and  $10^{-5}\ \text{M}$  CuPc (right). The scale shows the intensity of the  $1529\ \text{cm}^{-1}$  peak at each location.

The intensity maps showed that the surface of the sample prepared with  $10^{-5}\ \text{M}$  CuPc was more homogeneous than the one prepared with  $10^{-4}\ \text{M}$  CuPc (**Figure 4**). From this, it was hypothesized that at higher concentrations of CuPc, the formation of aggregates interferes with the adsorption of CuPc to the monolayer graphene, resulting in surface inhomogeneity.

To test this hypothesis, UV-Vis spectroscopy was employed to determine if and at which concentration these aggregates form. However, when attempting to measure the absorption spectra of the CuPC solution, it was found that CuPc was very poorly solubilized in dichloromethane. The expected absorption bands (Q-bands)<sup>9</sup> at 626 nm and 700 nm were not observed (**Figure 5**).

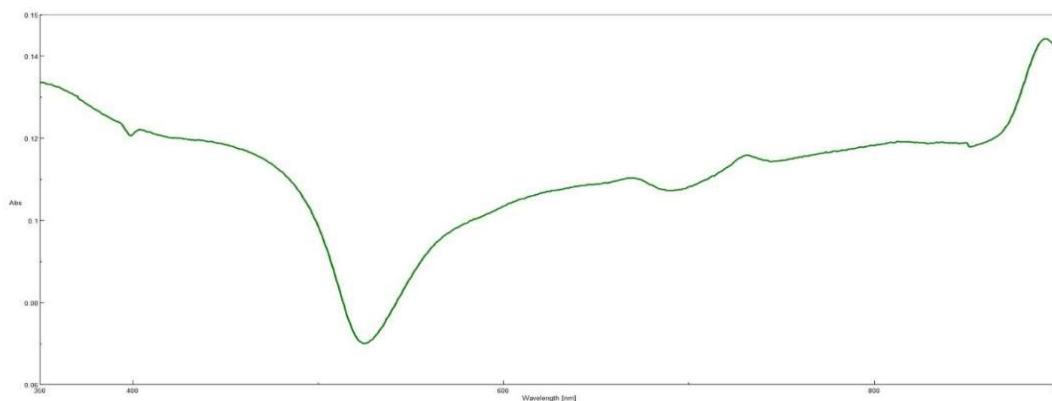


**Figure 5.** UV-Vis spectrum of  $10^{-5}\ \text{M}$  CuPc in dichloromethane. The lack of expected CuPc peaks indicated that CuPc had not been fully dissolved.

Upon closer examination, swirling the samples revealed particulates in the solution. Several other solvents were tested, particulates were still observed even with sonication. Without proper solubility, homogeneous coverage of CuPc was difficult to achieve by solution soaking process. To achieve better surface coverage of molecules on graphene, we decided to explore a more soluble derivative of CuPc.

### CuTTPc-coated graphene

Copper(II) 2,9,16,23-tetra-*tert*-butyl-29*H*,31*H*-phthalocyanine (CuTTPc) is a derivative of CuPc with *tert*-butyl groups attached to the four isoindole moieties. Because the dye scaffold is structurally similar to CuPc, the Raman spectrum of CuTTPc contains similar vibrational modes which arise from the macrocycle as well as the isoindole group (**Figure 6a**). CuTTPc has also been shown to interact with NO<sub>2</sub>, although this interaction is more likely to be a NO<sub>2</sub>-metal interaction<sup>10</sup> than a NO<sub>2</sub>-macrocycle interaction as is observed in CuPc.<sup>8</sup>

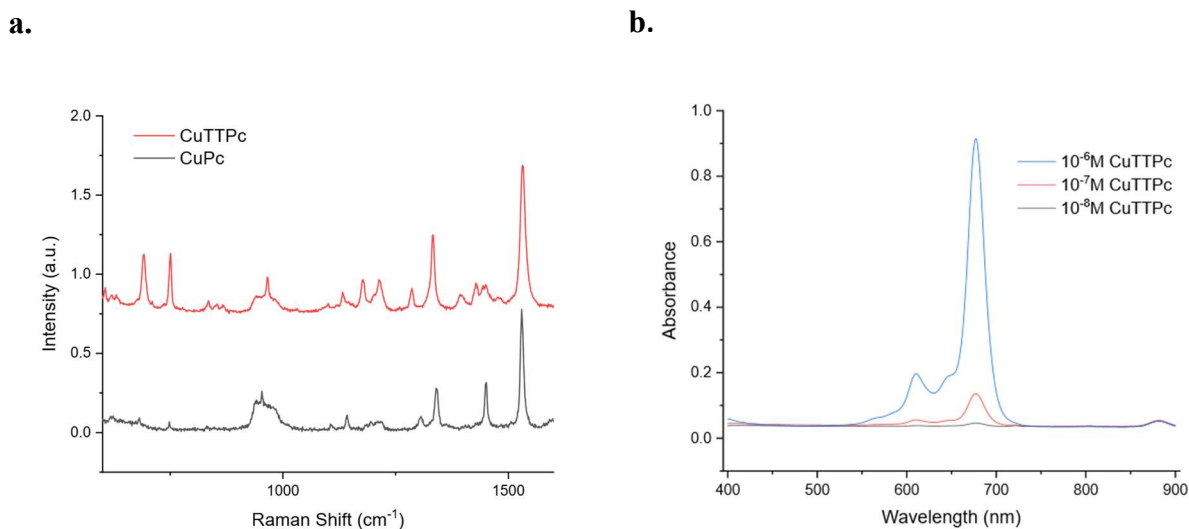


**Figure 6.** (a) Comparison of the Raman Spectra of CuPc and CuTTPc using 633 nm excitation. (b) Absorption spectrum of 10<sup>-5</sup>, 10<sup>-7</sup> and 10<sup>-8</sup> M CuTTPc in dichloromethane.

Solutions prepared with CuTTPc looked much different than those made with CuPc. The solution had a lighter color that faded gradually as the concentration was lowered, in contrast to the rapid loss of color for low concentrations of CuPc. To confirm that CuTTPc was soluble in dichloromethane and to test for evidence of aggregate formation, UV-Vis spectra were obtained. The absorption spectra of CuTTPc at different concentrations is shown in **Figure 6b**. Since the

bulky *tert*-butyl groups appended to the peripheral of the macrocycle successfully suppress the stacking of molecules in solution, no aggregate formation was observed even at high concentrations (**Figure 6b**).

The graphene enhanced Raman scattering was evident in graphene samples coated with CuTTPc. **Figure 7** shows comparison of the Raman spectrum of CuTTPc coated graphene silicon wafer and CuTTPc coated silicon wafer. Without graphene, the Raman modes of CuTTPc were almost unidentifiable. In the presence of graphene, the Raman modes are intense and clearly visible.

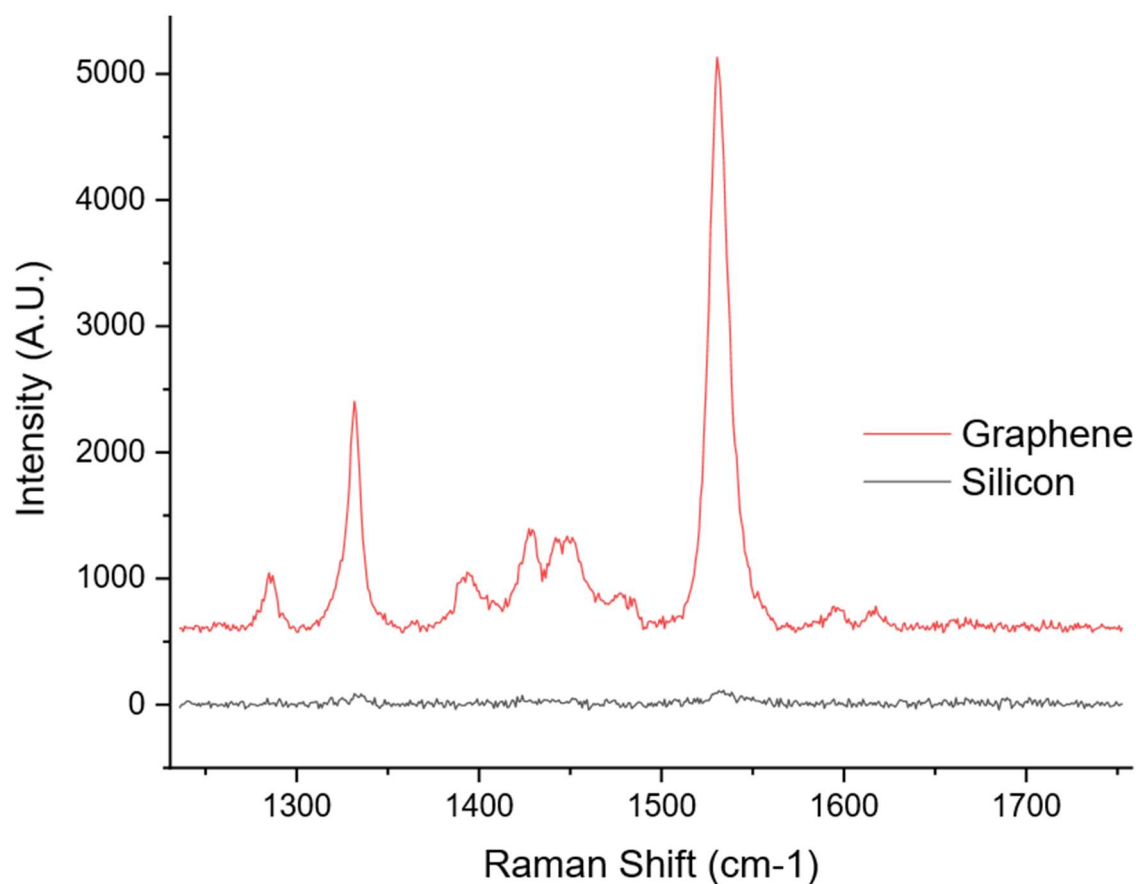


**Figure 7.** Demonstration of graphene enhancement effect of Raman scattering. The red spectrum is a CuTTPc-coated graphene silicon wafer. The black spectrum is a CuTTPc-coated silicon wafer. Spectra were obtained via 5-second exposure with 633nm laser. A Y-axis offset is applied for visibility.

To determine the optimal coating of CuTTPc molecules on graphene, we explored the concentration of CuTTPc in dichloromethane for solution soaking as well as the corresponding sample surface homogeneity. For this, we explored concentrations of CuTTPc in dichloromethane from  $1 \times 10^{-7}$  M to  $1 \times 10^{-4}$  M. Two samples of graphene on silicon wafer were used for each concentration, and four locations on each sample were selected at random and measured. The intensity **Figure 8** summarizes the average intensity and standard deviation of the most prominent Raman mode at  $1531 \text{ cm}^{-1}$ .

The optimal concentration was deemed to be the one with the greatest intensity and lowest variation in intensity.

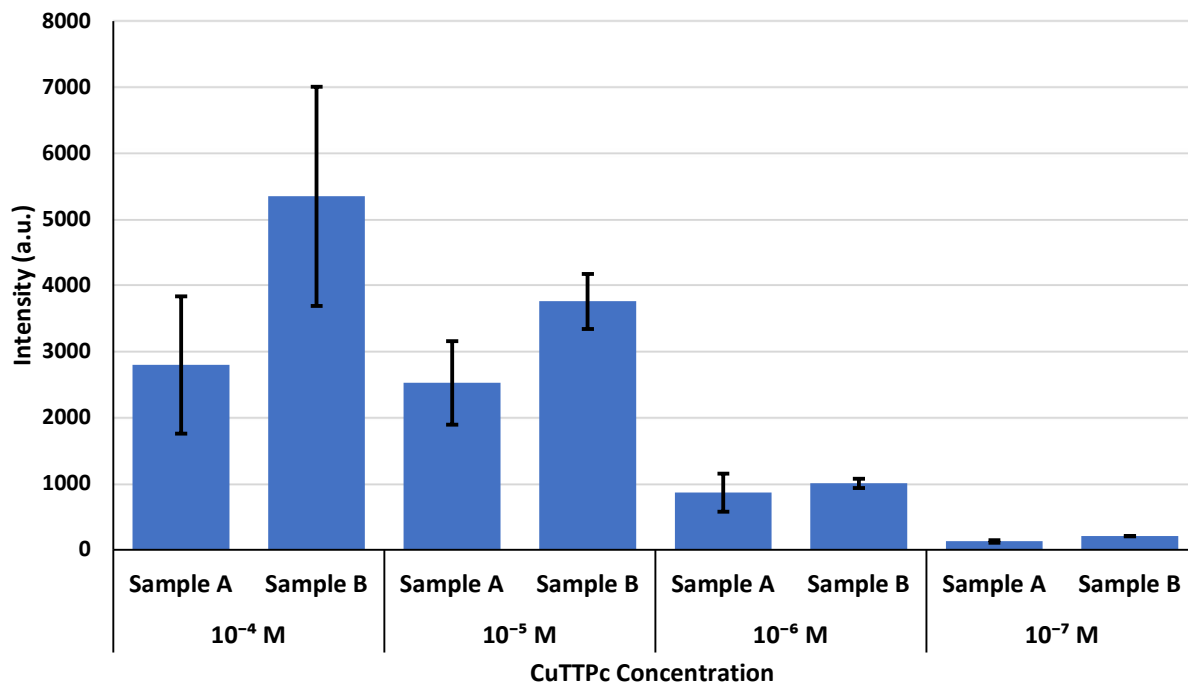


**Figure 8.** Surface homogeneity and intensity data for samples prepared with different concentrations of CuTTPc in dichloromethane. The average intensity of the  $1531 \text{ cm}^{-1}$  Raman mode at four locations with error bars indicating  $\pm 1$  standard deviation are shown.

The sample quality with shorter solution soaking times during the sample preparation step was evaluated. For this, graphene samples were immersed in a CuTTPc solution for 5 minutes instead of 1 hour. The average intensities of the Raman mode at  $1531 \text{ cm}^{-1}$  are summarized in **Figure 9**.

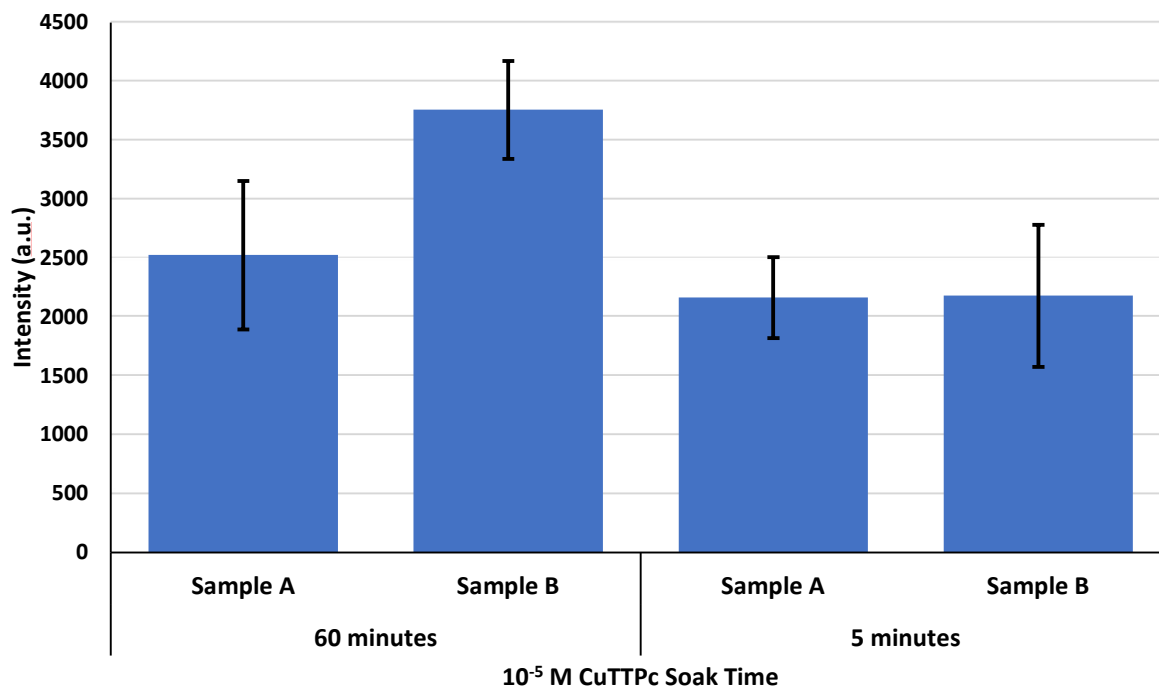


**Figure 9.** Surface homogeneity and intensity data for samples prepared with a 1-hour or a 5-minute soak in a  $10^{-5}$  M CuTTPc in dichloromethane solution. The average intensity of the  $1531\text{ cm}^{-1}$  Raman mode at three locations with error bars indicating  $\pm 1$  standard deviation are shown.

While the five-minute soak time resulted in less deviation in surface intensity measurements than the one-hour soak time, the average intensity was lower. To improve this, the 5-minute soak time was increased to 10 minutes for the samples used in the detection of  $\text{NO}_2$ .

### Initial Attempts at $\text{NO}_2$ Exposure

The first tests of the effect of  $\text{NO}_2$  exposure were conducted by exposing the CuPc samples to stream of 100 ppm  $\text{NO}_2$ . Graphene samples were coated with CuPc at a concentration of  $10^{-4}$  M in dichloromethane. Prior to  $\text{NO}_2$  exposure, the Raman spectra measured at seven separate locations were averaged together. After exposure to  $\text{NO}_2$  for a 10, 30, 60, or 120 second interval, the samples' Raman spectra were measured at seven different locations. We found that a correlation between Raman mode intensity change and  $\text{NO}_2$  exposure could not be determined due to large variation in the pre-exposure intensities across the different samples tested in these initial gas exposure experiments.

To obtain a more accurate reading of the interaction of nitrogen dioxide on CuPC Raman scattering, identical conditions between measurements needed to be ensured. Using the automatic stage on the Raman microscope, measurements at the same location on the functionalized graphene wafer before and after exposure can be made. To prevent the sample from moving on the stage, the graphene wafer was adhered to a glass microscope slide using double-sided tape. Reproducibility was verified by taking Raman measurements on a specific coordinate on the stage, before removing the sample and after placing it back on the stage.

Having achieved measurement location reproducibility, samples exposed to NO<sub>2</sub> still failed to give consistent intensity changes. We noticed that the time it took to expose a sample in the fume hood, return to the Raman spectrometer, locate the location of the initial measurement, focus it, and begin measuring was rather long and this varies each time a measurement is made. If the interaction of NO<sub>2</sub> is reversible, the expected Raman intensity changes could fade greatly within the few minutes it takes to begin measuring the Raman spectrum.

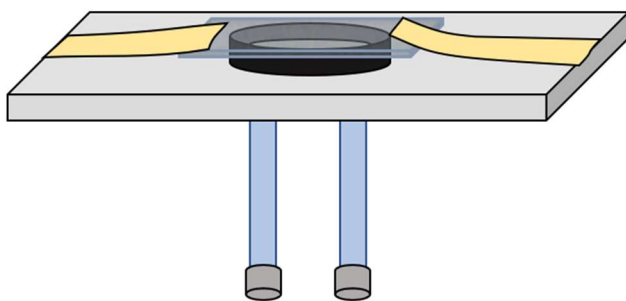


**Figure 10.** Enclosure designed to keep gas in contact with sample during measurement.

To prevent the lag in between NO<sub>2</sub> exposure and Raman measurement, we decided to place the samples in a sensing chamber shown in **Figure 10**. The enclosure allows the sample to be exposed to a controlled NO<sub>2</sub> atmosphere while Raman measurements are made. This was done by removing the glass cover on the chamber, taping the sample down in the center using double-sided tape, and replacing the glass slide cover. To establish the baseline intensity, we measured the Raman intensity at 1531cm<sup>-1</sup> every 10 seconds for 300 seconds. The sample would then be taken to a fume hood where the caps on the tubes at the bottom of the chamber were removed. One end would be attached to a NO<sub>2</sub> gas tank and the other left open. After 20 seconds of flowing NO<sub>2</sub> gas

through the enclosure, the gas was turned off, and the openings of the enclosure were sealed. The Raman spectra of the samples were measured. The results of this test are shown in **Figure 11**.

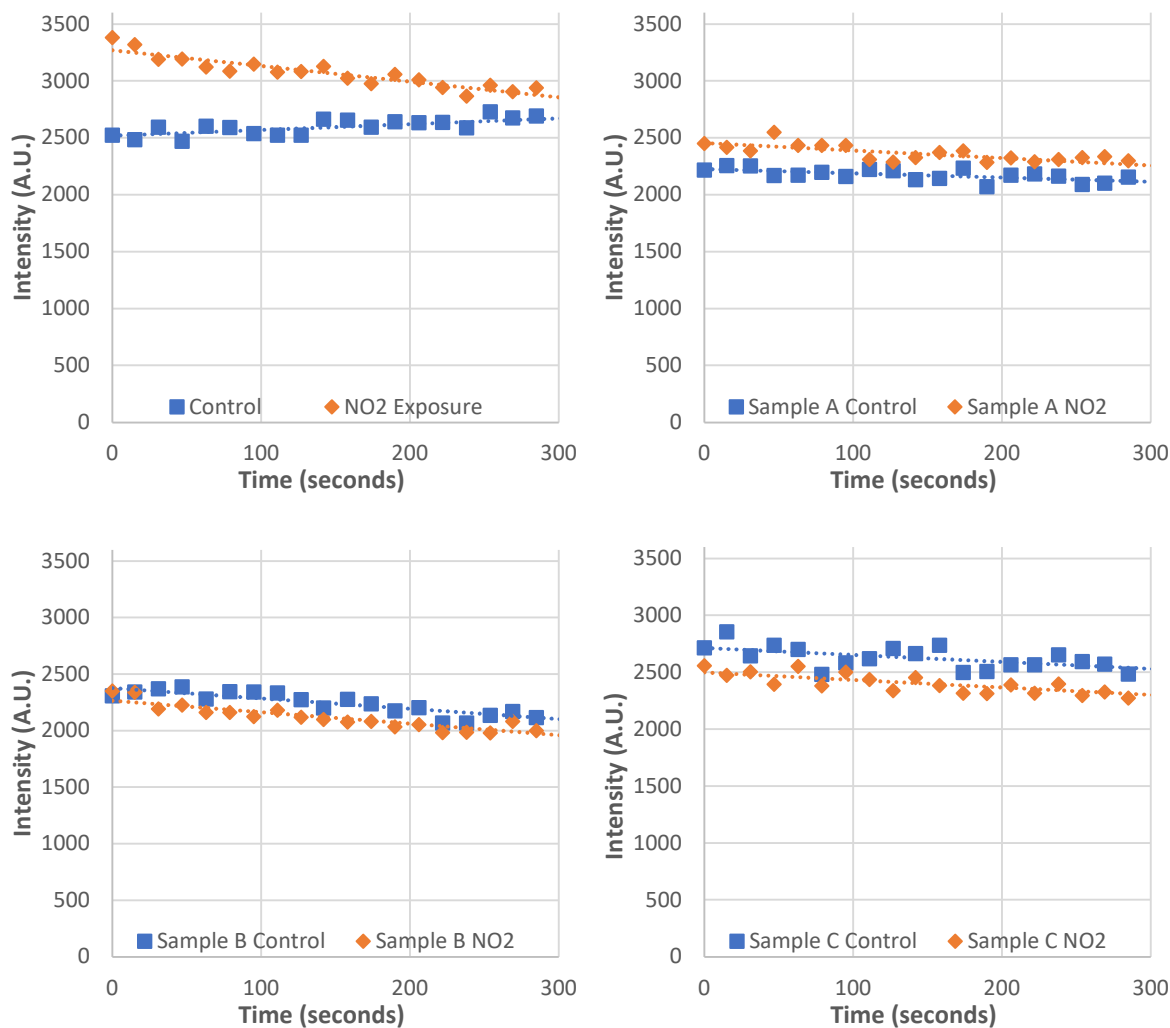


**Figure 11.** Exposure of CuTTPc coated graphene to 100 ppm NO<sub>2</sub>. Graphene samples were prepared by solution soaking in 10<sup>-5</sup> M CuTTPc in dichloromethane.

Although one of the samples showed a relatively stable baseline followed by a decrease in the intensity of the Raman mode at 1531 cm<sup>-1</sup> after exposure to NO<sub>2</sub>, the other samples showed a reduction in intensity during the baseline measurements and after exposure to NO<sub>2</sub>. We attribute the inconsistent Raman intensity due to sample movement and lag in time between exposure and Raman measurement. To improve the detection setup, we decided to build a more study enclosure that would allow us to measure the interaction of NO<sub>2</sub> in real time.



## Real-time Detection of NO<sub>2</sub>

The new enclosure has a gas chamber mounted on a plastic slide with a tight-fitting lid that has a glass window that allows light to pass through. Gas can be fed into and flow-out of the chamber through the inlet and outlet at the bottom. Graphene coated with different concentrations of CuTTPc were tested with the new sensing enclosure shown in **Figure 12**. Four graphene samples were prepared using  $1.12 \times 10^{-4}$ ,  $1.12 \times 10^{-5}$ ,  $1.12 \times 10^{-6}$ , and  $1.12 \times 10^{-7}$  M of CuTTPc in dichloromethane. The four samples were soaked for 10 minutes in 1 mL of each solution. The samples were then removed with tweezers and dried horizontally under a stream of nitrogen gas. The results of these tests are shown in **Figures 13–15**.

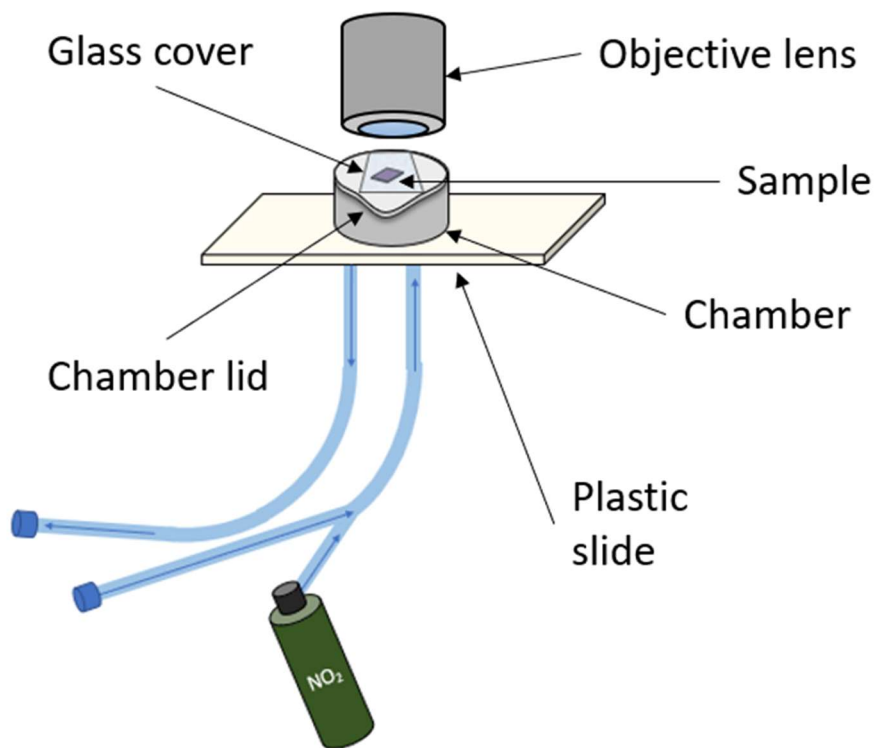


**Figure 12.** Construction of real-time NO<sub>2</sub> sensing enclosure.

As expected, the initial Raman scattering intensities of CuTTPc increase with increasing concentrations of CuTTPc in the sample preparation. All samples responded to NO<sub>2</sub> with a reduction in Raman intensities upon exposure. The reduction in signal intensity increases as the amount of CuTTPc coated on graphene increases, from  $10^{-6}$  to  $10^{-4}$  M. Samples prepared with a

$10^{-3}$  M solution exhibited lower intensity reduction upon exposure, possibly due to the formation of multilayer of CuTTPc in concentrated solutions. Since samples prepared with  $10^{-4}$  M CuTTPc had the largest response or the largest reduction in intensity of the  $1531\text{ cm}^{-1}$  mode, we proceeded with our study with samples prepared at this concentration.

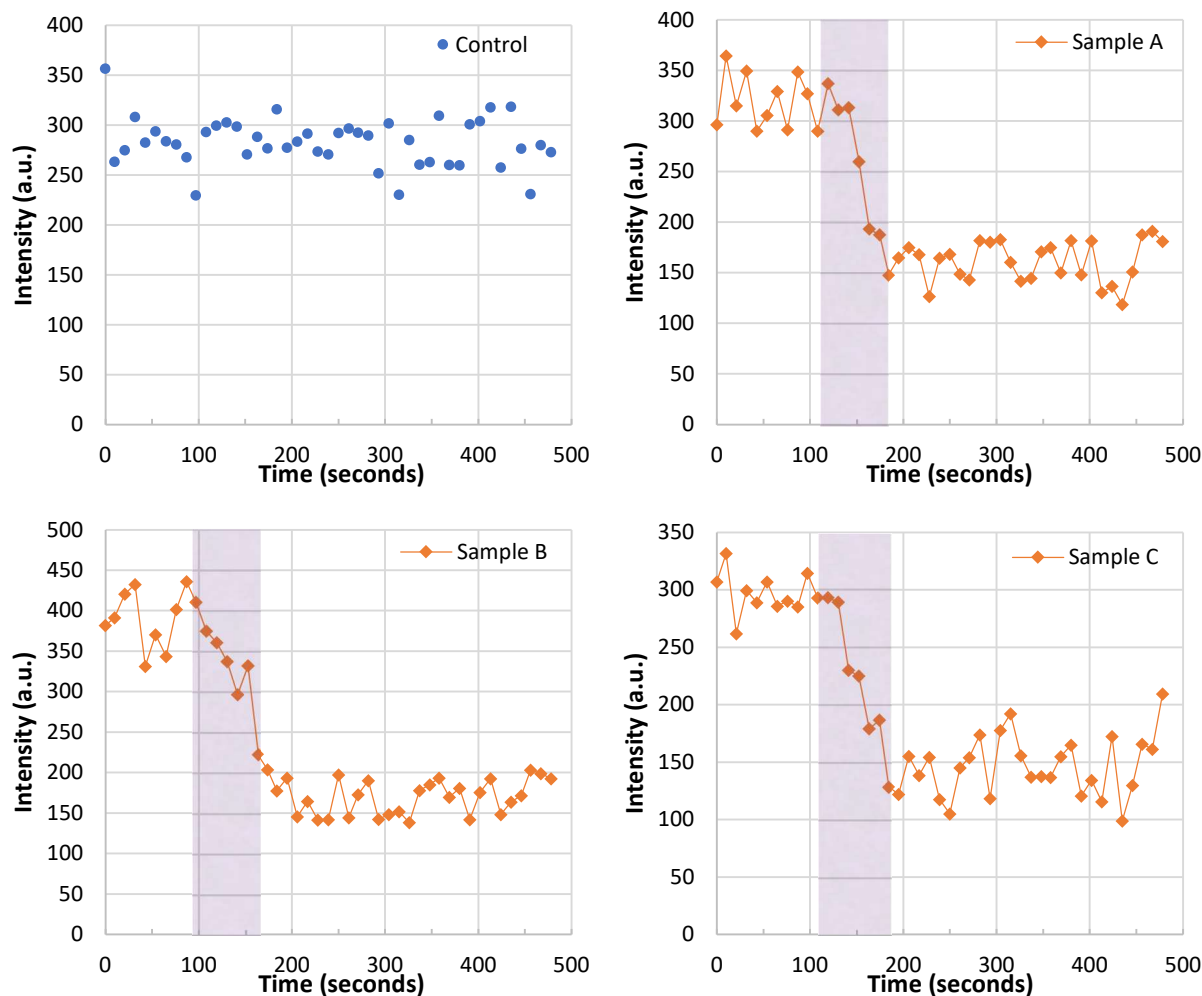


**Figure 13.** Intensity of Raman mode  $1531\text{ cm}^{-1}$  upon exposure to 100 ppm  $\text{NO}_2$  in air. Samples were prepared by solution soaking in  $10^{-6}$  M CuTTPc in dichloromethane. Three samples were measured. Shaded areas indicate  $\text{NO}_2$  exposure.

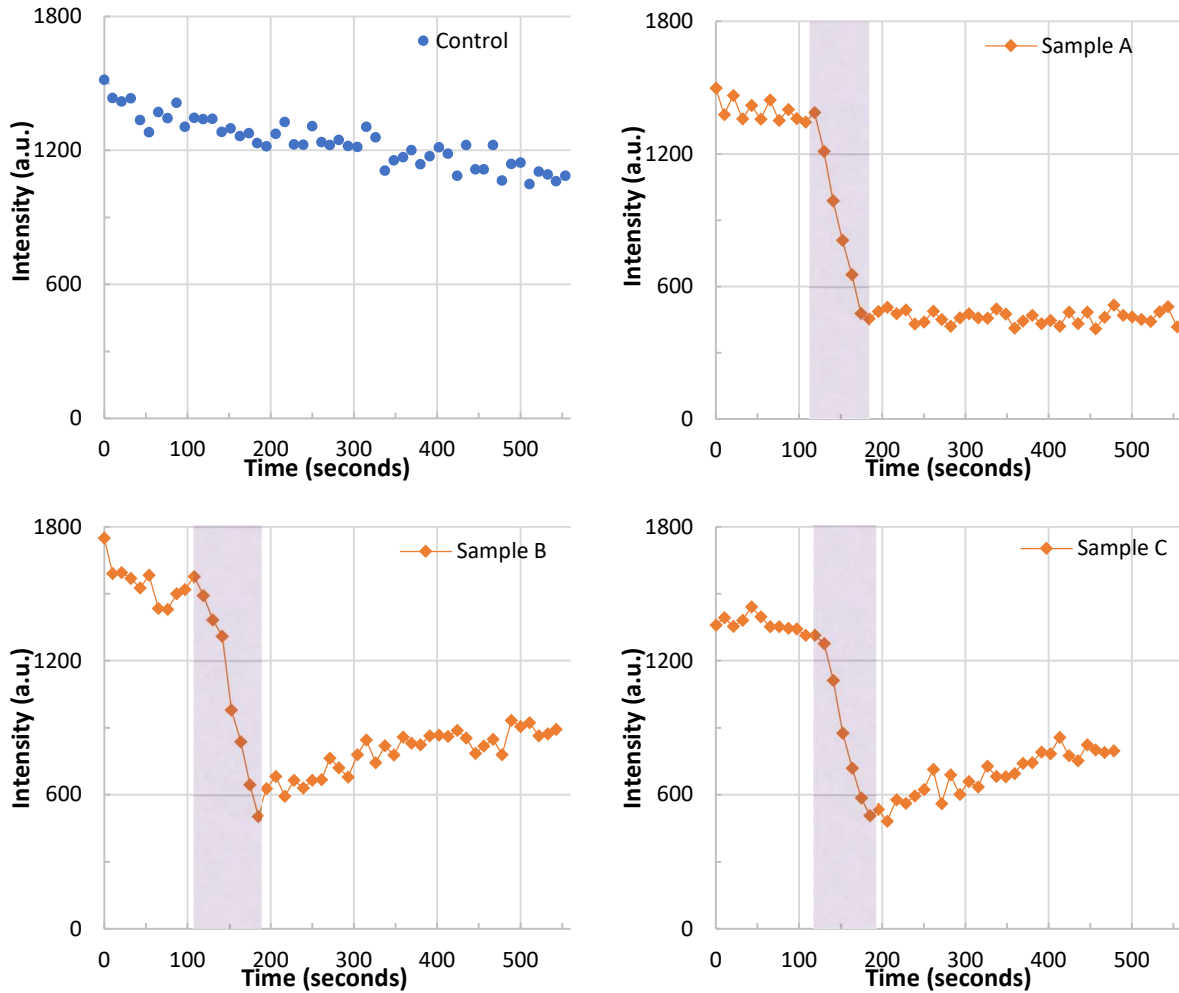


**Figure 14.** Intensity of Raman mode 1531 cm<sup>-1</sup> upon exposure to 100 ppm NO<sub>2</sub> in air. Samples were prepared by solution soaking in 10<sup>-5</sup> M CuTTPc in dichloromethane. Three samples were measured. Shaded areas indicate NO<sub>2</sub> exposure.

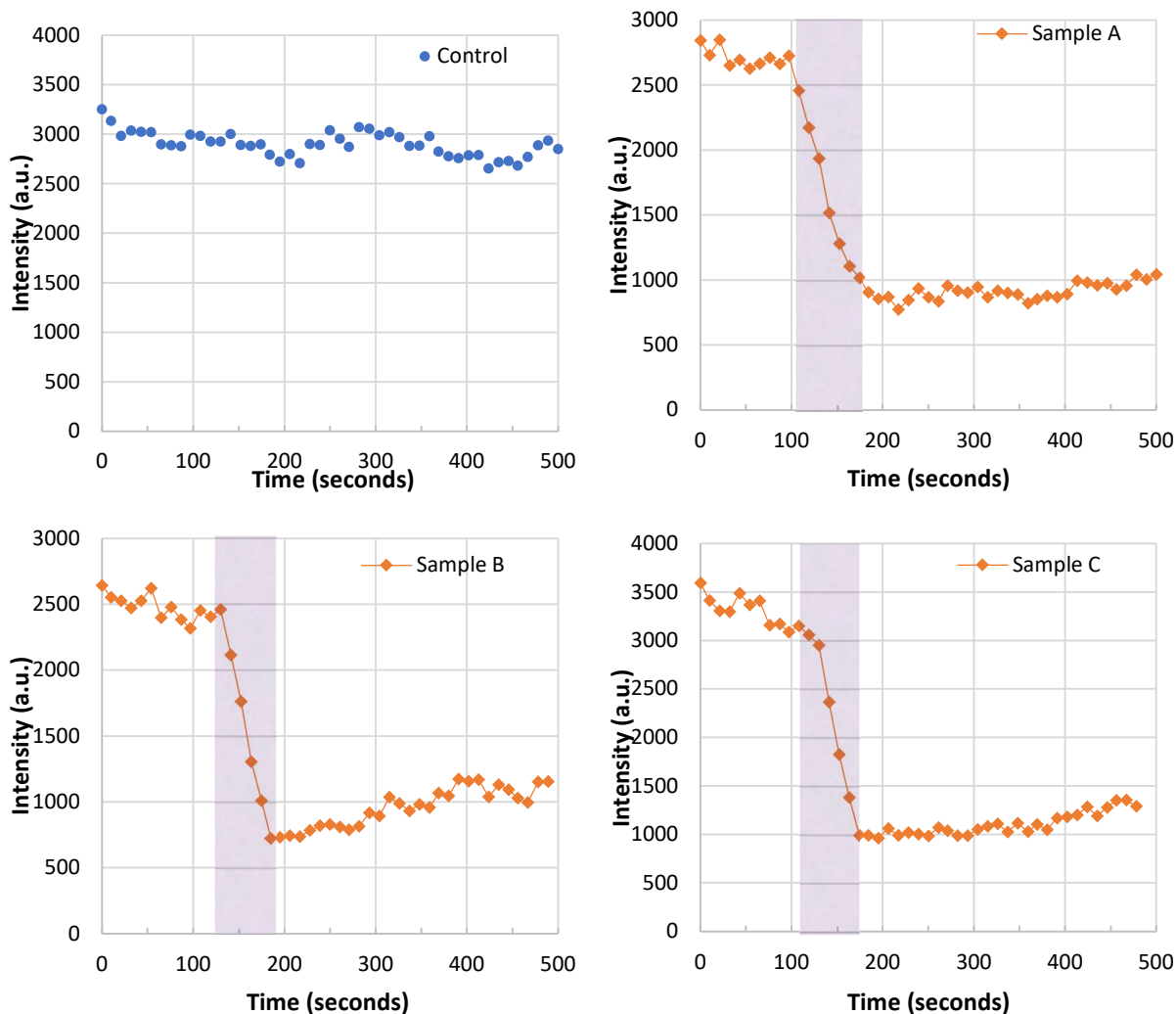


**Figure 15.** Intensity of Raman mode 1531 cm<sup>-1</sup> upon exposure to 100 ppm NO<sub>2</sub> in air. Samples were prepared by solution soaking in 10<sup>-4</sup> M CuTTPc in dichloromethane. Three samples were measured. Shaded areas indicate NO<sub>2</sub> exposure.

Further testing was done using this setup at lower concentrations of NO<sub>2</sub> gas in order to construct a calibration curve. This was done by diluting the NO<sub>2</sub> calibration gas with compressed air using a Y-joint in the air hoses. By increasing the flow rate of compressed air in the mixture (using a flow meter), the concentration of NO<sub>2</sub> could be diluted. The humidity level of the compressed air was measured and found to be zero. Samples were exposed to 50 ppm and 10 ppm NO<sub>2</sub>, in addition to the 100 ppm tests conducted earlier. The results were plotted as percentage decrease compared to the initial intensity (**Figure 16**).

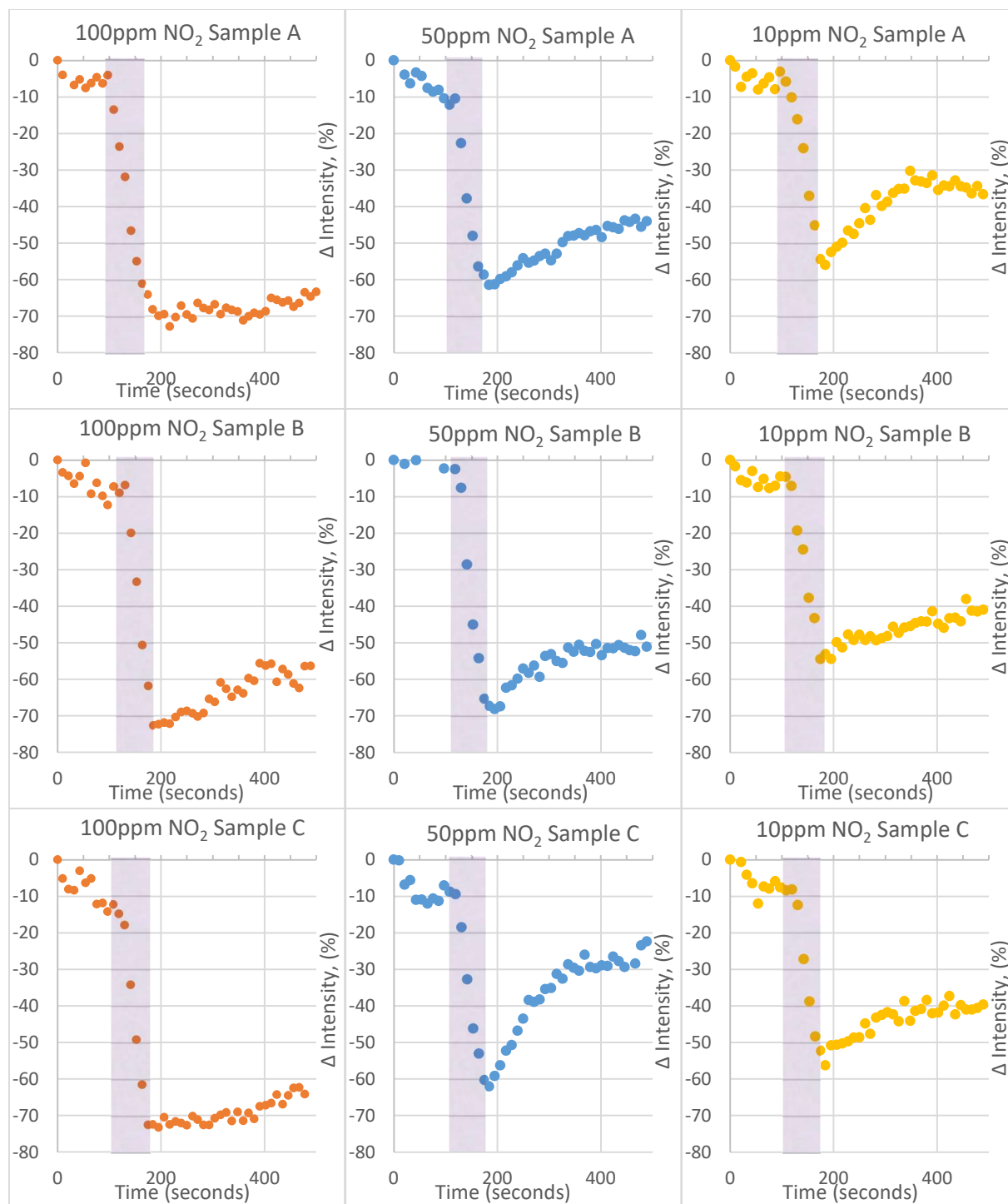


**Figure 16.** Response of CuTTPc coated graphene to various concentrations of NO<sub>2</sub>. All samples were prepared by solution soaking in 10<sup>-4</sup> M CuTTPc in dichloromethane. Shaded areas indicate NO<sub>2</sub> exposure.

The average decrease in intensity was averaged for each concentration of gas exposure. Based on this calibration curve, predictions can be made about the expected concentration of gas given the decrease in Raman scattering intensity—allowing the sensor to function quantitatively. The calibration curve is shown in **Figure 17**.

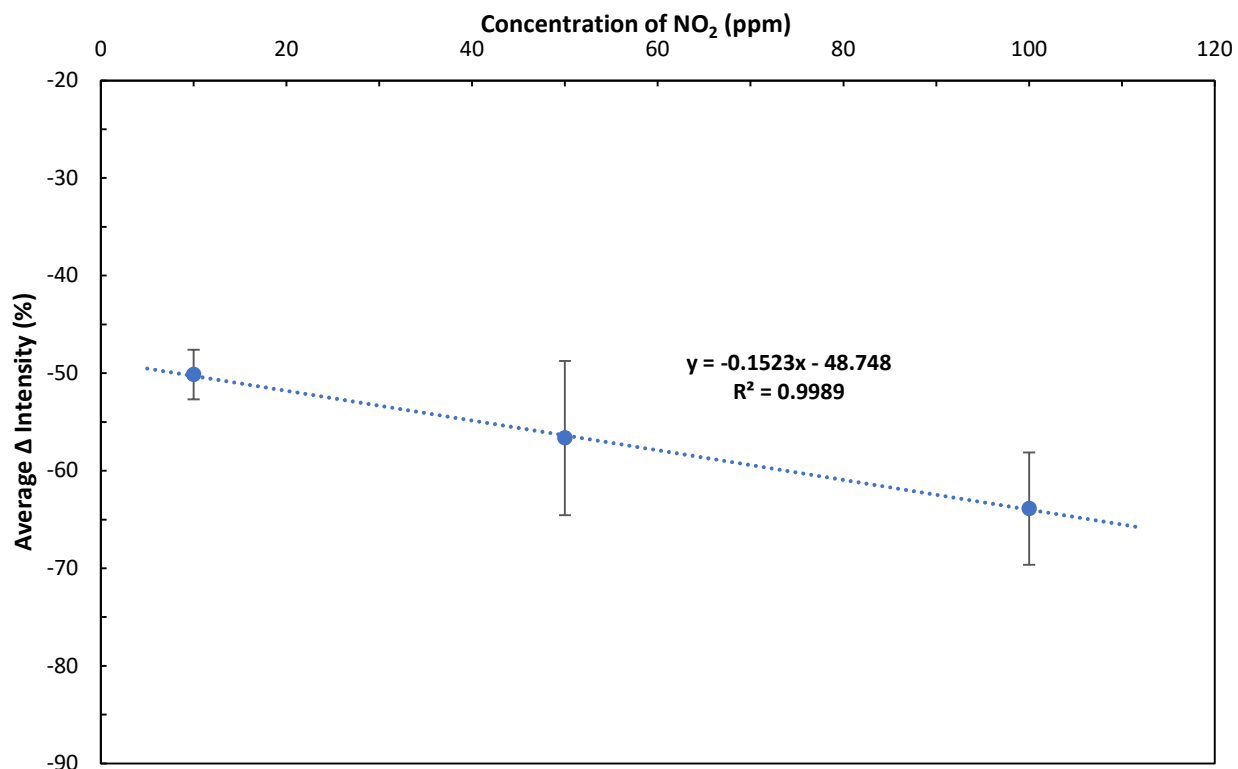


**Figure 17.** Calibration curve for NO<sub>2</sub> quantification. Error bars show  $\pm 1$  standard deviation.

Currently, the upper boundary of exposure is 100 ppm, as the calibration gas tank supplies 100 ppm at a fixed flow rate of 0.25 L/min. Lower concentration of NO<sub>2</sub> was obtained by dilution with air. However, our current setup limited us to go down to about 10 ppm of NO<sub>2</sub>. Concentrations lower than 10 ppm would require a different setup for supplying the gas mixture. The limit of detection can be improved by increasing the signal-to-noise ratio. Using a sensing chamber with a glass rather than plastic base should reduce vibrations and flexing, resulting in lower noise levels.

The final tests conducted with the real-time NO<sub>2</sub> sensing enclosure were designed to determine the reusability of the sensor. Samples were prepared as before. Baselines were collected for 5 minutes, after which they were exposed to 50 ppm and 10 ppm NO<sub>2</sub> for 1 minute. After exposure, the sample was left under compressed air flow to return to the baseline before being exposed to NO<sub>2</sub> again for another minute. The results of this test are shown in **Figure 18**.

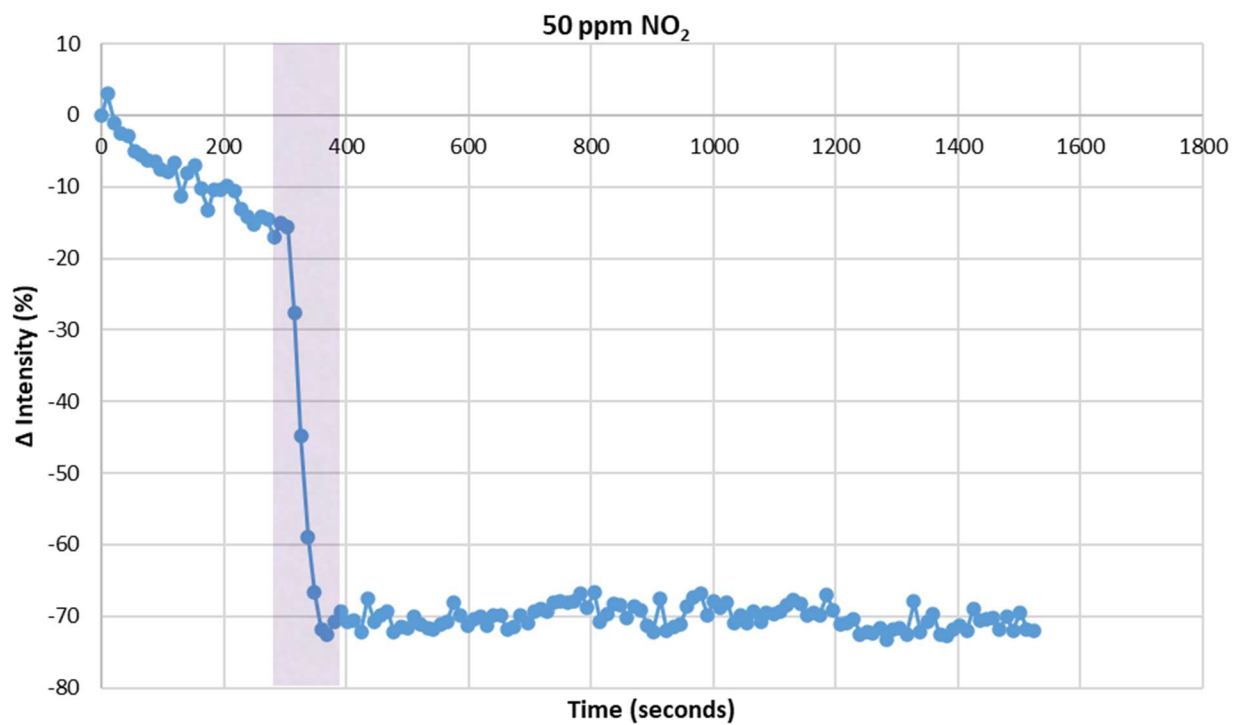
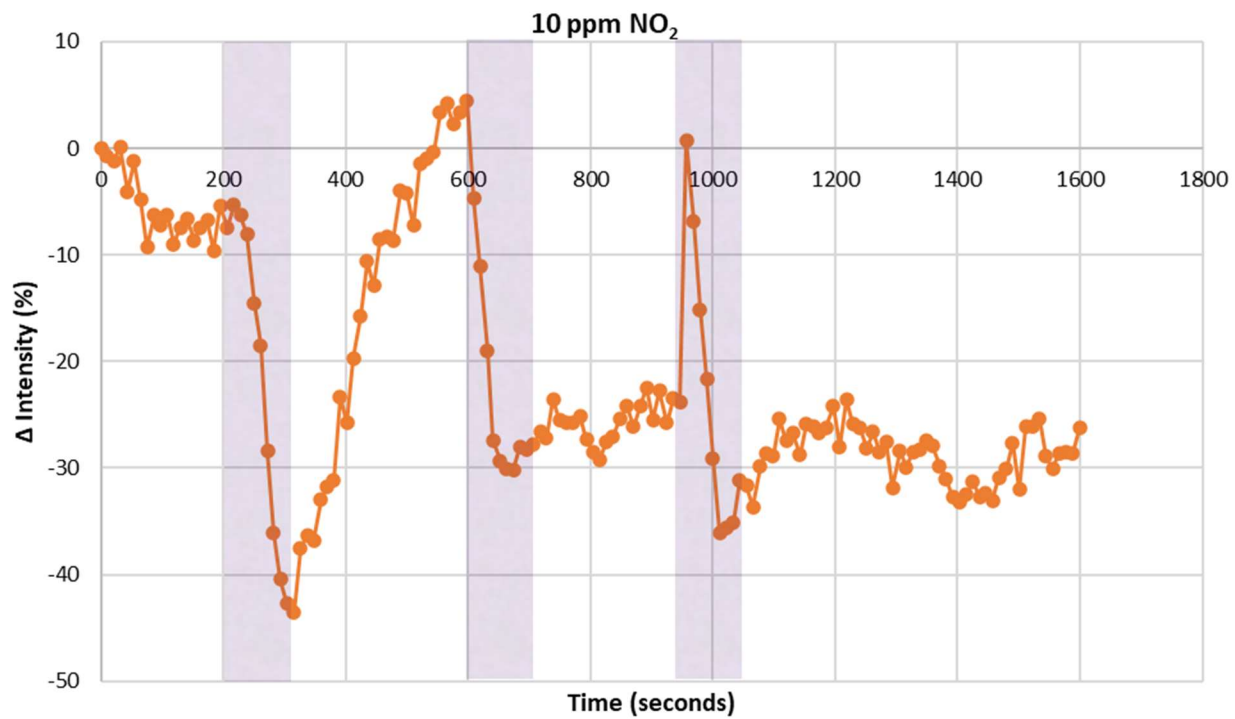


**Figure 18.** Raman intensity at 1531 cm<sup>-1</sup>. Intensity is recorded as a percent change from the initial. Shaded areas indicate NO<sub>2</sub> exposure.

Based on this test, it seems that exposure to lower concentrations of NO<sub>2</sub> allow for more complete recovery, whereas higher concentrations result in a more permanent decrease in Raman scattering intensity. Likewise, after the second exposure, recovery is slow and incomplete, even for exposure to 10 ppm NO<sub>2</sub>.

### Sensing Mechanism

While a reduction in Raman intensity during exposure to nitrogen dioxide was established in the previous section, the mechanism by which this reduction occurred remained unknown. It has been reported that both CuPc and CuTTPc form charge transfer complex with NO<sub>2</sub> with NO<sub>2</sub> being the electron acceptor.<sup>7,10</sup> However, NO<sub>2</sub> is also known to induce p-doping in graphene through charge transfer.<sup>11</sup>

The extended-range Raman spectra of CuTTPc on graphene before and after exposure to 100 ppm NO<sub>2</sub> showed that all of the Raman modes of CuTTPc (vibration modes associated with the macrocycle and isoindole groups) decreased in intensity (**Figure 19**). This observation is consistent with the decrease in Raman mode intensity observed when cobalt phthalocyanine on graphene is exposed to oxidizing gas O<sub>2</sub>.<sup>11</sup>

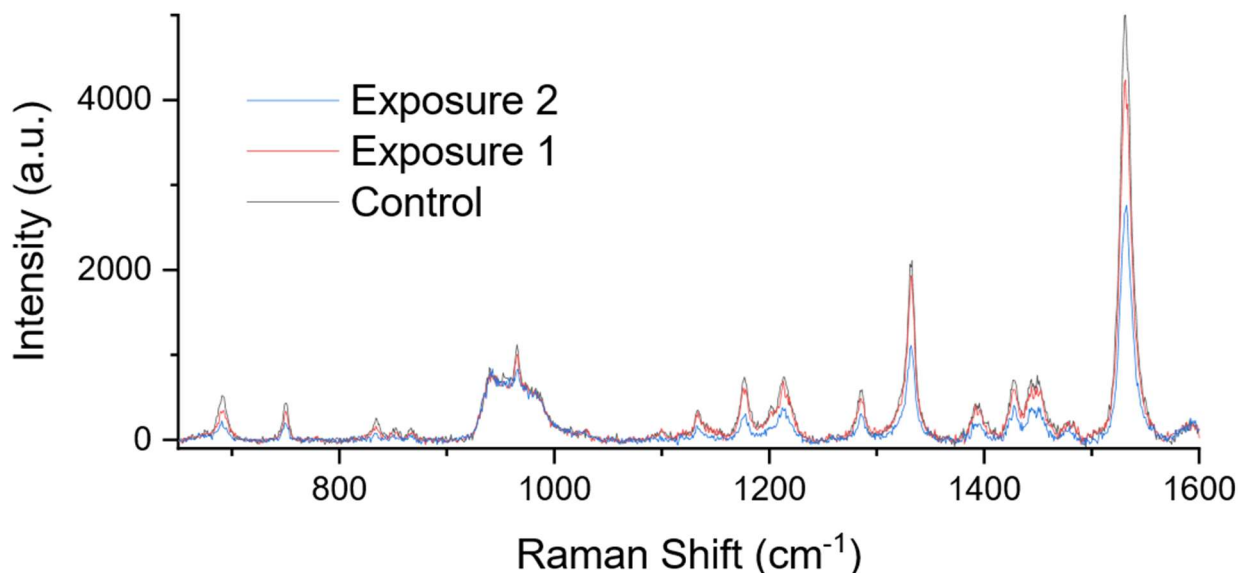


**Figure 19.** Full-range Raman spectra of sample prepared with 10<sup>-4</sup> CuTTPc. The control was acquired before NO<sub>2</sub> exposure. Exposures 1 and 2 were recorded back-to-back with continuous exposure to 100 ppm NO<sub>2</sub>. Each spectrum took about 30 seconds to record.



To determine if NO<sub>2</sub> is interacting with graphene or CuTTPc, a new sample will be created by depositing CuTTPc on a silicon wafer, then depositing monolayer graphene on top of that. The magnitude of intensity change after exposure to NO<sub>2</sub> can be compared to the sensors prepared with CuTTPc on top of graphene. Due to its extremely thin structure, Raman scattering bands for molecules located underneath a graphene layer can still be observed. However, since NO<sub>2</sub> cannot come in direct contact with CuTTPc, observation of a CuTTPc signal decrease with this sensor design will provide evidence that NO<sub>2</sub>-graphene interactions contribute to the sensing mechanism.

## **Conclusion and Future Work**

Through the course of this project, the construction of a functional NO<sub>2</sub> sensor on the basis of GERS was demonstrated. The sensor was shown to be capable of both detection and quantification of NO<sub>2</sub>. The Raman mode intensity reduction correlates with the concentration of NO<sub>2</sub> in air. The sensors showed a linear response from 10–100 ppm.

Currently, the limitation in experimental instrumentation limited the range of gas concentrations that could be tested. Lower concentrations were limited by the airflow required to dilute the 100-ppm calibration gas. Future experiments using mass flow controllers would be needed to determine the limit of detection for these sensors.

A major issue encountered in the construction of this sensor was the lack of surface homogeneity. While the solution soaking method of functionalization was the simplest, it creates very inconsistent coating of molecules on graphene. Using another method of deposition such as vacuum or Langmuir-Blodgett monolayer deposition should result in a significantly more homogenous coating. However, these deposition methods require expensive specialized equipment that was not available for this initial study. The covalent method of functionalization, as discussed in the introduction to this paper, could also be explored as a method of creating a more homogeneous and durable sensor.

To determine how selective are the sensors responding to NO<sub>2</sub>, a selectivity study would need to be conducted. This would be done by exposing the sensor to other gases commonly found in the same environments as NO<sub>2</sub>, such as nitrogen, oxygen, moisture, carbon dioxide, etc. Future experiments will also be conducted to determine whether NO<sub>2</sub> is interacting with graphene or CuTTPc or both.

## References:

- (1) Skoog, D. A.; Holler, F. J.; Crouch, S. R. Raman Spectroscopy. In *Principles of instrumental analysis*; Cengage Learning, 2018; pp 437–453.
- (2) Pilot, R.; Signorini, R.; Durante, C.; Orian, L.; Bhamidipati, M.; Fabris, L. A Review on Surface-Enhanced Raman Scattering. *Biosensors*. MDPI June 1, 2019. <https://doi.org/10.3390/bios9020057>.
- (3) Huang, S.; Ling, X.; Liang, L.; Song, Y.; Fang, W.; Zhang, J.; Kong, J.; Meunier, V.; Dresselhaus, M. S. Molecular Selectivity of Graphene-Enhanced Raman Scattering. *Nano Lett* **2015**, *15* (5), 2892–2901. <https://doi.org/10.1021/nl5045988>.
- (4) Ling, X.; Xie, L.; Fang, Y.; Xu, H.; Zhang, H.; Kong, J.; Dresselhaus, M. S.; Zhang, J.; Liu, Z. Can Graphene Be Used as a Substrate for Raman Enhancement? *Nano Lett* **2010**, *10* (2), 553–561. <https://doi.org/10.1021/nl903414x>.
- (5) Ling, X.; Huang, S.; Deng, S.; Mao, N.; Kong, J.; Dresselhaus, M. S.; Zhang, J. Lighting Up the Raman Signal of Molecules in the Vicinity of Graphene Related Materials. *Acc Chem Res* **2015**, *48* (7), 1862–1870. <https://doi.org/10.1021/ar500466u>.
- (6) National Center for Biotechnology Information. *PubChem Compound Summary for CID 3032552, Nitrogen Dioxide*. PubChem.
- (7) Basova, T. V.; Kol'tsov, E. K.; Igumenov, I. K. Spectral Investigation of Interaction of Copper Phthalocyanine with Nitrogen Dioxide. *Sens Actuators B Chem* **2005**, *105* (2), 259–265. <https://doi.org/10.1016/j.snb.2004.06.007>.
- (8) Chia, L. S.; Du, Y. H.; Palale, S.; Lee, P. S. Interaction of Copper Phthalocyanine with Nitrogen Dioxide and Ammonia Investigation Using X-Ray Absorption Spectroscopy and Chemiresistive Gas Measurements. *ACS Omega* **2019**, *4* (6), 10388–10395. <https://doi.org/10.1021/acsomega.8b02108>.
- (9) Ling, X.; Moura, L. G.; Pimenta, M. A.; Zhang, J. Charge-Transfer Mechanism in Graphene-Enhanced Raman Scattering. *Journal of Physical Chemistry C* **2012**, *116* (47), 25112–25118. <https://doi.org/10.1021/jp3088447>.
- (10) Battisti, D.; Aroca, R. *Reversible Adsorption on a Single Langmuir-Blodgett Monolayer*; 1992; Vol. 114. <https://pubs.acs.org/sharingguidelines>.
- (11) Yavari, F.; Castillo, E.; Gullapalli, H.; Ajayan, P. M.; Koratkar, N. High Sensitivity Detection of NO<sub>2</sub> and NH<sub>3</sub> in Air Using Chemical Vapor Deposition Grown Graphene. *Appl Phys Lett* **2012**, *100* (20). <https://doi.org/10.1063/1.4720074>.